GEOLOGICA CARPATHICA, DECEMBER 2009, 60, 6, 535–543 doi: 10.2478/v10096-009-0039-7

Experimental interactions of Slovak bentonites with metallic iron

MAREK OSACKÝ[1], MIROSLAV HONTY[1], JANA MADEJOVÁ[2], THOMAS BAKAS[3] and VLADIMÍR ŠUCHA[1]

[1]Department of Geology of Mineral Deposits, Comenius University, Mlynská dolina G, 842 15 Bratislava, Slovak Republic; osacky@fns.uniba.sk; honty@fns.uniba.sk; sucha@fns.uniba.sk
[2]Institute of Inorganic Chemistry, Slovak Academy of Sciences, Dúbravská cesta 9, 845 36 Bratislava, Slovak Republic; jana.madejova@savba.sk
[3]Department of Physics, University of Ioannina, 45110 Ioannina, Greece; tbakas@cc.uoi.gr

(Manuscript received December 18, 2008; accepted in revised form June 25, 2009)

Abstract: The experimental stability of four bentonites and one K-bentonite from Slovak deposits in the presence of iron was studied to simulate the possible reactions of clays (bentonite barrier) in the contact with Fe containers in a nuclear waste repository. The batch experiments were performed at 60 °C for 30 and 120 days in aerobic conditions. The reaction products were examined by XRD, FTIR, and Mössbauer spectroscopies and CEC (cation exchange capacities) were determined. Reaction solutions were analysed for selected elements using AAS (atomic absorption spectrometry). The results show that bentonites do not interact equally with metallic iron. Bentonites from the Jelšový Potok, Kopernica and Lieskovec deposits reacted similarly whereas the interaction between the bentonite from Lastovce and the iron was less intensive. The lower reactivity of the bentonite from Lastovce can be explained by its low content of smectite. During iron-clay interactions the iron was consumed and Fe oxides (magnetite, lepidocrocite) were formed. Decrease of the smectite diffraction peaks intensity and CEC values during the experiments show rather the rearrangement of the original smectite crystals than dissolution of smectite. In the K-bentonite from the Dolná Ves deposit where the mixed-layer illite-smectite is present instead of smectite, the dissolution of illite-smectite was observed along with the neoformation of smectite. The structure of illite-smectite deteriorated more than the structure of smectites which suggests that this mixed-layer illite-smectite is much less stable in the presence of iron than smectites.

Key words: nuclear waste repository, clay stability, bentonite, illite-smectite, smectite, magnetite, iron.

Introduction

It is envisaged that high-level nuclear waste (HLW) will be disposed of in underground repositories. Several current designs for the future geological disposal of HLW suggest the use of a multibarrier system with two basic components — a host rock and an engineered barrier. The engineered barrier comprises the respective metallic containers filled with radioactive waste and barrier made up of bentonite blocks. The metallic containers could be made up of iron or copper (JNC 2000; Push 2001, 2003; Thorsager & Lindgren 2004; SKI 2005; Arthur et al. 2005). To predict the long-term properties of the components in the designed barriers of HLW repository it is essential to study their interactions. This paper focuses on the interactions between bentonitic clays and iron.

This rather complex topic has been the subject of several research projects in the last years. Börgesson et al. (2002) assume that the container will corrode anaerobically and that the principal corrosion product will be magnetite (Smart et al. 2002). Nevertheless, oxidizing conditions are likely to occur before closure of the repository and other iron compounds than magnetite may also be formed at this stage.

Several experimental studies of iron-clay interactions showed the systematic destabilization of the initial clay material and the subsequent crystallization of reaction products (Guillaume et al. 2003, 2004; Lantenois et al. 2005; Wilson et al. 2006; Perronnet et al. 2007). The nature of these reaction products depends on experimental conditions such as temperature and the nature of the initial clay material. Fe-rich chlorite species are newly-formed after interaction of smectite with iron at higher temperature (300 °C) (Guillaume et al. 2003), whereas Fe-rich serpentine-like species are synthesized at lower temperatures (80 °C) (Haber 2000; Lantenois 2003; Perronnet 2004). Lantenois et al. (2005) observed that dioctahedral smectites are destabilized while trioctahedral smectites are essentially unaffected under similar experimental conditions during iron-clay interactions. They also found that smectite destabilization by the interaction with iron is enhanced by structural Fe^{3+} in the smectite, by the interlayer Na^{+} cations, and by the alkaline pH, respectively. However taking into account the results of Lantenois et al. (2005), Perronnet (2004) and Perronnet et al. (2007) it is clear that some additional parameters may also have an impact on the reaction rate of the iron-smectite interactions. Apparently the smectite layer charge and the textural and energetic surface heterogeneities of smectite crystals may play a role.

The clay-water ratio should be taken into considerations when the experimental results are interpreted. For instance Müller-Vonmoos et al. (1991) reviewed by Madsen (1998) found no significant changes in the bentonite samples after interaction with iron and magnetite at 80 °C for 29 weeks, when no additional water was present in the reaction system. The

aim of the present work was to investigate the stability of smectite and illite-smectite in the presence of iron to simulate the possible reactions of bentonites in contact with a Fe container in a nuclear waste repository. Most of the experimental studies of iron-clay interactions were performed under oxygen-free conditions. There is a lack of experimental data regarding iron-clay interactions in aerobic conditions, however oxidizing conditions are likely to occur before closure of the nuclear waste repository. For these reasons our experiments were carried out in the aerobic environment. In addition we bring here the first results of the stability of mixed-layer illite-smectite in the presence of iron.

Materials, experimental setting and analytical methods

Four bentonites from Slovak deposits at Jelšový Potok (J45), Kopernica (K45), Lieskovec (L45), Lastovce (La45) and one K-bentonite from the Dolná Ves (DV45) deposit were used for experiments (Fig. 1). All the bentonites are commercially available products technologically treated by drying, grinding and size separated to <45 μm. The iron represents a 99% pure metallic Fe^0 powder with particle size of 10 μm.

The mixtures of iron with bentonite in redistilled water (2 g/10 g/106 ml) were prepared in polyethylene (PE) bottles in fully aerobic conditions. After mixing the starting materials, the PE bottles were closed and the experiments were conducted at 60 °C for 30 and 120 days. It means that the treatment of the samples before and after the experiments was conducted in fully aerobic conditions. However, the experiments themselves were conducted in semi-aerobic conditions. Once the plastic containers were closed no additional oxygen was available. The initial volume of free air in the bottles was approximately 195 ml, the estimated molar ratio of atmospheric oxygen to iron was about 0.047.

At the end of the reactions the samples were cooled to room temperature and opened in air. After centrifugation the solution was filtered (0.45 μm) and pH, Eh and conductivity were subsequently measured. The filtered solutions were analysed for selected elements (Si, Al, Ca, Na, Mg, K, Fe) using AAS (atomic absorption spectrometry). The solid fraction was dried at 60 °C overnight, ground and analysed. The fine fraction (<2 μm) of samples before and after experiments was separated by sedimentation and used for analyses as well.

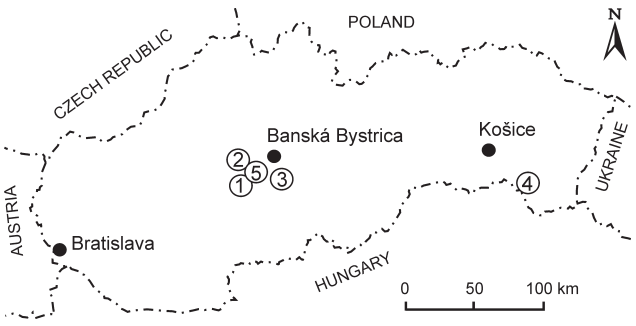

Fig. 1. Location of: **1** — Jelšový Potok, **2** — Kopernica, **3** — Lieskovec, **4** — Lastovce, **5** — Dolná Ves deposits.

X-ray diffraction (XRD) analyses of oriented (air-dried and ethylene glycolated) and random specimens were carried out using a Phillips PW 1710 diffractometer (35 kV, 20 mA) with CuKα radiation and a graphite monochromator. All samples were scanned with a step 0.02° 2 theta and count time 0.80 s per step over a measuring range of 2 to 50° 2 theta.

Quantitative XRD analysis was performed by RockJock modelling. RockJock is a computer program (Eberl 2003) that determines quantitative mineralogy in powdered samples by comparing the integrated X-ray diffraction intensities of individual minerals in complex mixtures to the intensities of an internal standard (ZnO). Samples (3.000 g) were mixed with internal standard ZnO (0.333 g) and wet ground in a McCrone Micronizing Mill for 5 minutes (Środoń et al. 2001). Random specimens were scanned with a step of 0.02° 2 theta and count time 2 s per step over measuring range of 4 to 65° 2 theta. The X-ray data were entered into the RockJock computer program and the mineral compositions of the samples were calculated.

The quantitative XRD analysis (RockJock) of samples after the experiment was not performed because not all the minerals present in bentonites are listed in the RockJock mineral database. Only minerals listed in the RockJock mineral database can be quantified. The quantitative amount of SiO_2 forms (cristobalite, volcanic glass) was determined by RockJock from XRD patterns as well.

The relative amount of the residual iron after the experiment was estimated from the intensity of diffraction peaks of iron in XRD patterns. We assumed that more intensive iron diffraction peaks indicated higher amounts of residual iron (i.e. lower consumption) and less intensive peaks indicated lower amounts of the iron (i.e. higher consumption) after the experiment.

The Fourier transform infrared (FTIR) spectra in the middle region (4000–400 cm^{-1}) were obtained using a Nicolet Magna 750 spectrometer with a DTGS detector and a KBr beam splitter. The KBr pressed-disc technique (1 mg of sample and 200 mg of KBr) was used for the transmission measurements. Discs were heated in a furnace overnight at 150 °C to minimize the water adsorbed on KBr and the clay sample.

Mössbauer spectra were obtained at liquid nitrogen temperatures (80 K) using a Wissel spectrometer equipped with an Oxford Variox 316 cryostat. A ^{57}Co source was moved in constant acceleration mode. Velocity calibration was carried out with respect to the centre of a Fe foil spectrum at room temperature. The spectra were deconvoluted with a least-squares computer program assuming Lorentzian line-shapes.

The complex of copper(II) triethylentetramine $[Cu\ Trien]^{2+}$ was used for determination of cation exchange capacity (CEC) of the samples. The 0.01 M solution of the complex $[Cu\ Trien]^{2+}$ was prepared according to Meier & Kahr (1999). 100 mg of samples were added to 50 ml of distilled water and 10 ml solution of $[Cu\ Trien]^{2+}$. The suspensions were dispersed by an ultrasonic treatment for 5 minutes, filtrated and the concentration of Cu(II) complex was determined by UV-VIS spectrophotometry (Cary 100, Varian) at 578 nm (Meier & Kahr 1999). The amount of adsorbed $[Cu\ Trien]^{2+}$ was determined using molar absorption coeffi-

cient $\varepsilon = 0.245\ mol^{-1} \cdot dm^3 \cdot cm^{-1}$ (Kaufhold & Dohrmann 2003) and the CEC values were calculated.

Element contents were determined by the flame atomic absorption spectrometry (AAS) method. Si and Al were measured in acetylene-nitrous oxide flame (AAS Perkin Elmer Model 5000), Ca, Na, Mg, K and Fe in acetylene-air flame (AAS Perkin Elmer Model 1100). Lanthanum was added (c(La) = 1 g/l) for the determination of Ca and Mg, Fe was measured with deuterium background correction.

Results

X-ray diffraction

All the starting samples were analysed by XRD. Samples J45, K45, L45 and La45 have similar mineral compositions while sample DV45 is different. The non-clay minerals quartz, K-feldspar, cristobalite and volcanic glass (for explanation of how the volcanic glass was detected see discussion) were found in samples K45, L45 and La45 (Figs. 2, 3).

The principal layer silicate in bentonites is smectite with small amounts of kaolinite and biotite (Figs. 2, 3). The presence of (060) peak at ~0.149 nm indicates dioctahedral smectite. The sample La45 contains the lowest amount of smectite, the highest amounts of cristobalite, volcanic glass and a small amount of calcite compared with the samples J45, K45 and L45 (Table 1). The mineral composition of sample DV45 is dominated by quartz, K-feldspar and volcanic glass. Instead of smectite, the mixed-layer illite-smectite is present with non-expandable (illite) layers forming about 68 %, and traces of biotite and kaolinite (Fig. 4). The RockJock quantitative XRD data are listed in Table 1. The smectite content in bentonites varies between 81 and 42 %. The illite-smectite content of DV45 is 34 %. The residual iron (0.202 nm) was present together with newly-formed magnetite (0.253 nm) in the XRD

Table 1: Mineralogical compositions (in wt. %) of starting samples (fractions <45 μm) determined by RockJock computer program.

Minerals	Sample				
	J45 (wt.%)	K45 (wt. %)	L45 (wt. %)	La45 (wt. %)	DV45 (wt. %)
Quartz	7	7	12	14	47
Plagioclase	0	0	0	5	0
K-feldspar	5	7	10	6	2
Biotite	0	1	0	0	3
Kaolinite	2	0	6	2	1
Smectite	81	77	56	42	0
Cristobalite	0	1	4	6	0
Volcanic glass	5	7	12	21	13
Calcite	0	0	0	4	0
Illite-smectite	0	0	0	0	34

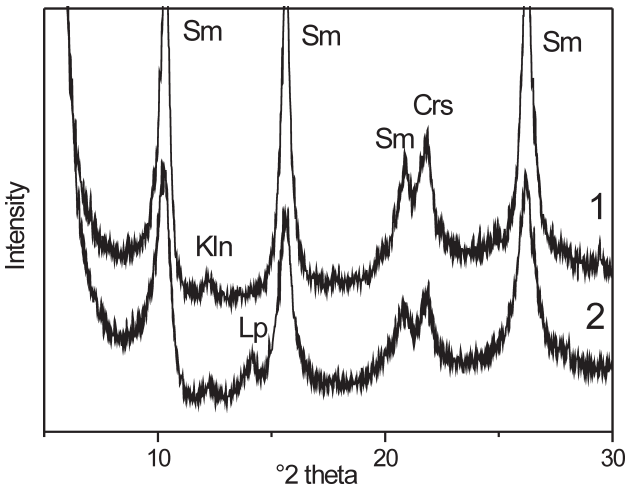

Fig. 3. XRD patterns of the oriented (<2 μm, ethylene glycolated) samples of La45. **1** — starting bentonite, **2** — after 30 days of iron-bentonite interactions. **Sm** — smectite, **Kln** — kaolinite, **Crs** — cristobalite, **Lp** — lepidocrocite.

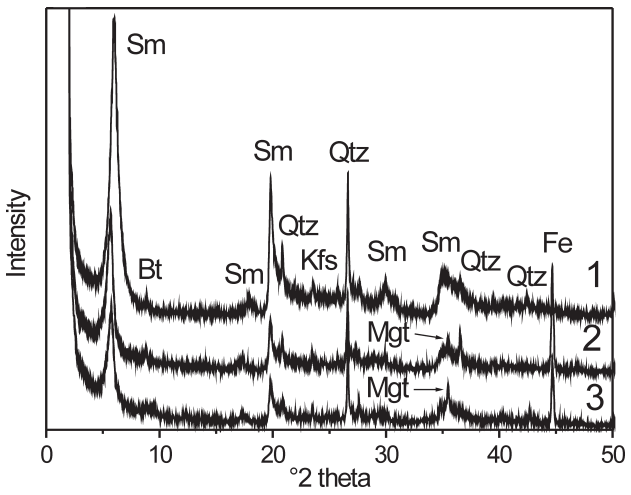

Fig. 2. XRD patterns of random specimens of bentonite K45 (fractions <45 μm). **1** — starting bentonite, **2** — after 30 days of iron-bentonite interactions, **3** — after 120 days of iron-bentonite interactions. **Sm** — smectite, **Bt** — biotite, **Qtz** — quartz, **Kfs** — K-feldspar, **Mgt** — magnetite, **Fe** — iron.

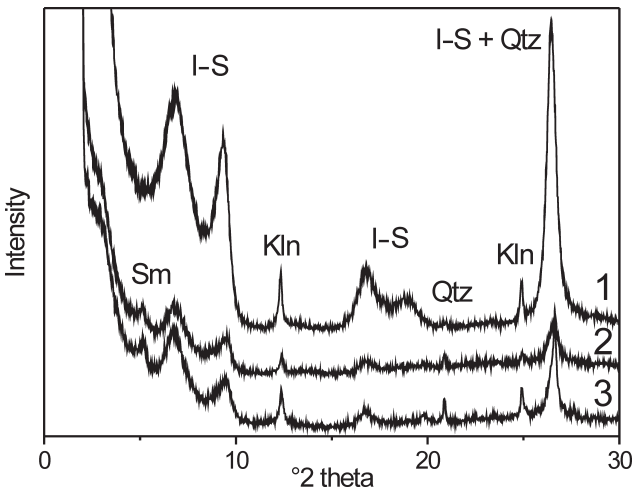

Fig. 4. XRD patterns of the oriented (<2 μm, ethylene glycolated) samples of K-bentonite DV45. **1** — starting K-bentonite, **2** — after 30 days of iron-bentonite interactions, **3** — after 120 days of iron-bentonite interactions. **I–S** — illit-smectite, **Kln** — kaolinite, **Qtz** — quartz, **Sm** — smectite.

patterns of randomly oriented specimens of samples J45, L45, K45 and DV45 after the interactions conducted for 30 and 120 days (Fig. 2). The decrease of intensity of the iron diffraction peak in XRD patterns after 120 days with respect to the 30 day patterns, indicate the higher consumption of iron in experiments with longer duration. The intensity of the diffraction peaks of quartz and feldspars decreased significantly after the experiments in all samples. The sample La45 reacted with iron after 30 days differently with respect to the samples mentioned above. The diffraction peaks of cristobalite and calcite decreased significantly during the experiments but the peaks of iron did not change significantly and no magnetite was formed. It indicates that iron was much less consumed (oxidized) during iron-bentonite interactions and it is still present in its original oxidation state (Fe^0). This finding was also confirmed by Mössbauer spectroscopy (Table 2). Instead of magnetite a small amount of lepidocrocite (0.627 nm) was formed (Fig. 3).

The XRD patterns of oriented specimens (<2 μm) also showed that the intensity of the smectites diffraction peaks decreased in all samples. Their position did not change during the experiments (Fig. 3).

K-bentonite from Dolná Ves (sample DV45) reacted in a similar way to smectitic bentonites (J45, L45 and K45), however the illite-smectite peaks decreased more significantly than the smectite peaks of bentonites. Interestingly a peak of newly formed smectite was observed at low two-theta degrees of the EG saturated patterns (Fig. 4).

FTIR spectroscopy

The IR spectra of samples J45, K45, La45 and L45 after 30 days of iron interactions at 60 °C showed no differences with respect to the original IR spectra J45, K45, La45, L45 (Fig. 5c,d). No significant changes were observed in the shape and position of bands from samples before and after the experiments. No changes in the structural OH groups and Si–O vibrations indicate that no structural changes occurred in the tetrahedral and octahedral sheets of smectites during iron interactions after 30 days in samples J45, K45, La45 and L45. The potential formation of Fe oxyhydroxides during iron-clay interactions cannot be detected by IR spectroscopy, because the absorption bands of these Fe compounds are usually overlapped by more intense bands of smectite.

The most evident differences were observed between the IR spectra of sample DV45 and DV45 after 30 days (Fig. 5a,b). The intensity of the AlAlOH band at 915 cm^{-1} decreased, the AlMgOH band at 848 cm^{-1} disappeared and the intensity of the quartz doublet at 800 and 779 cm^{-1} increased (Fig. 5a,b).

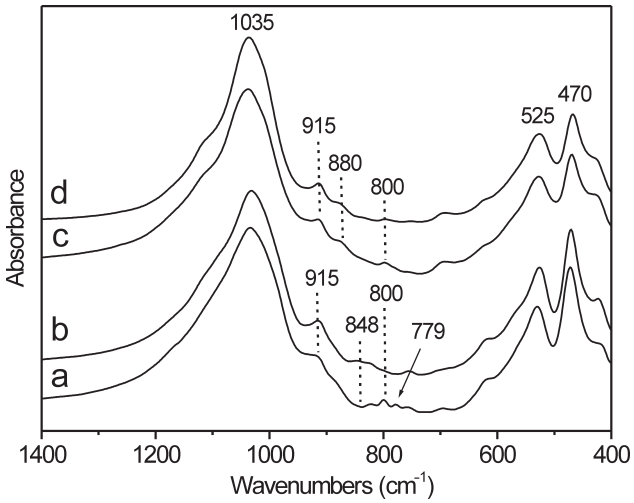

Fig. 5. FTIR spectra of samples (fractions <2 μm) before and after iron interactions. **a** — DV45 after 30 days, **b** — DV45, **c** — L45 after 30 days, **d** — L45.

Table 2: Hyperfine parameters (B_{hf} — magnetic hyperfine field, IS_{Fe} — isomer shift, **QS** — quadrupole splitting) and relative areas (%) of spectral components from the Mössbauer spectra of samples after 30 days of iron-bentonite interactions, measured at 80 K.

Sample		Bhf (T)	ISFe (mm/s)	QS (mm/s)	Area (%)	Determination
J45	Doublet 1	0	0.43	0.69	41	Montmorillonite + Fe-oxides
	Sextet 1	51.5	0.5	–0.1	16	Hematite
	Sextet 2	47.5	0.51	–0.05	13	Al-hematite
	Sextet 3	43.3	0.47	–0.16	13	Goethite?
	Sextet 4	34.4	0.11	–0.02	17	Metallic iron
L45	Doublet 1	0	0.47	0.69	40	Montmorillonite + Fe-oxides
	Sextet 1	49.6	0.5	–0.07	15	Hematite
	Sextet 2	46.2	0.47	–0.06	10	Al-hematite
	Sextet 3	42.1	0.45	–0.17	13	Goethite?
	Sextet 4	34.6	0.12	–0.01	12	Metallic iron
K45	Doublet 1	0	0.48	0.72	28	Montmorillonite + Fe-oxides
	Sextet 1	51.9	0.51	–0.14	11	Hematite
	Sextet 2	47.6	0.5	–0.05	8	Al-hematite
	Sextet 3	43.3	0.49	–0.16	7	Goethite?
	Sextet 4	34.4	0.11	–0.01	46	Metallic iron
DV45	Doublet 1	0	0.46	0.8	31	Montmorillonite + Fe-oxides
	Sextet 1	51.8	0.51	–0.1	24	Hematite
	Sextet 2	48	0.52	–0.06	14	Al-hematite
	Sextet 3	43.5	0.5	–0.18	13	Goethite?
	Sextet 4	34.4	0.1	–0.01	18	Metallic iron
La45	Doublet 1	0	0.54	0.68	9	Montmorillonite
	Sextet 4	34.4	0.11	0.01	91	Metallic iron

The spectral changes of the sample DV45 reflected OH group dehydroxylation and release of the central atoms (Al, Mg) from the octahedral sheet of illite-smectite.

Mössbauer spectroscopy

The Mössbauer spectra of samples J45, K45, DV45, L45 and La45 after iron interaction at 60 °C for 30 days were taken at liquid nitrogen temperatures. The prominent central doublet in the spectra of all samples is characteristic of Fe(III) in octahedral coordination with no magnetic ordering, indicating that the Fe is bound primarily in the phyllosilicate structure (Figs. 6–10). The sextets in the spectra of all samples are attributed to the octahedral Fe(III) of Fe (oxyhydr)oxides and to the Fe(0) of residual metallic Fe, all with magnetic ordering (Figs. 6–10).

The Mössbauer spectrum of the sample J45 shows that 41 % of the Fe is bound in paramagnetic phases (Fig. 6, Table 2). Based on the hyperfine parameters (isomer shift, quadrupole splitting; Table 2), this doublet is assigned to phyllosilicate, montmorillonite which is the most abundant mineral in the sample J45. Because of relatively high amount of the total Fe (41 %) contributing to the doublet signal, we assume that the doublet could be attributed to iron atoms bound in small particle-size or Al-substituted Fe (oxyhydr)oxides also. Both Al substitution and small particle-size often lead to the decrease of the magnetic ordering temperature of Fe (oxyhydr)oxides (Golden et al. 1979; Murad 1988, 1989; Friedl & Schwertmann 1996; Betancur et al. 2004). The Mössbauer spectrum of the sample J45 contains four sextets at 80 K (Fig. 6). Based on the hyperfine parameters (Table 2), two sextets assigned to hematite and Al-hema-

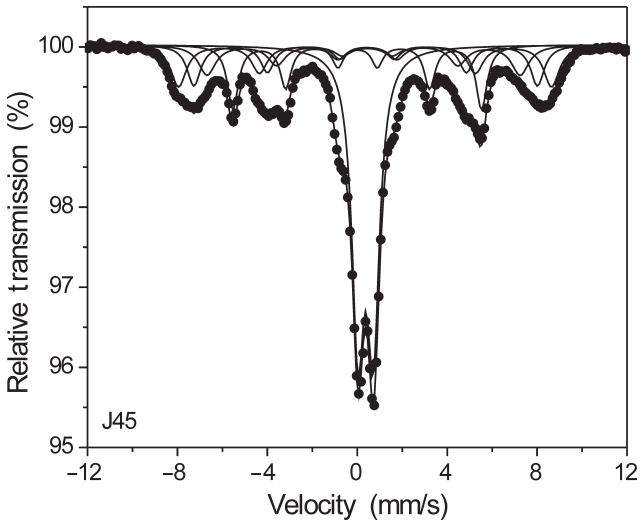

Fig. 6. Mössbauer spectrum of sample J45 after 30 days of iron-bentonite interactions, measured at 80 K.

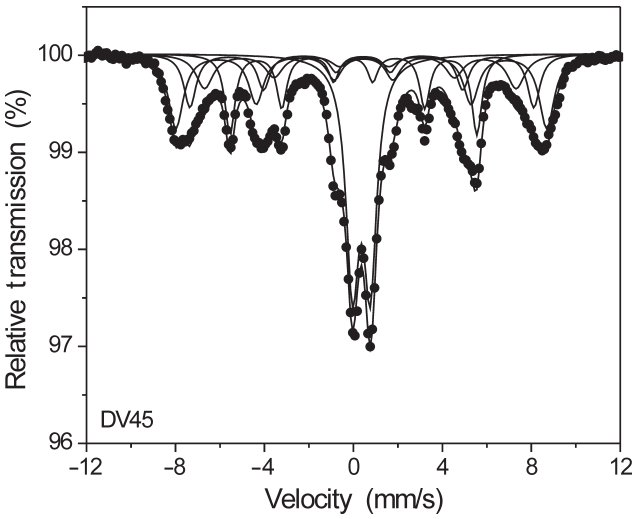

Fig. 8. Mössbauer spectrum of sample DV45 after 30 days of iron-bentonite interactions, measured at 80 K.

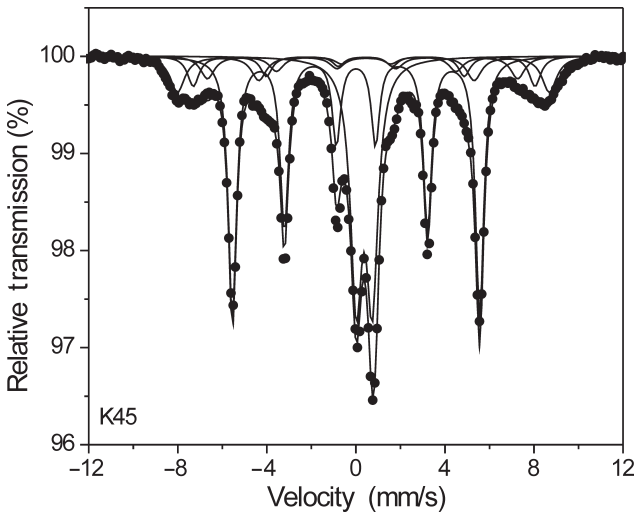

Fig. 7. Mössbauer spectrum of sample K45 after 30 days of iron-bentonite interactions, measured at 80 K.

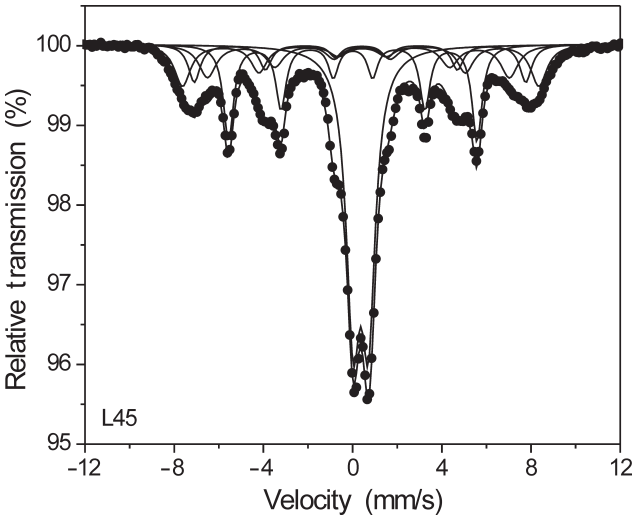

Fig. 9. Mössbauer spectrum of sample L45 after 30 days of iron-bentonite interactions, measured at 80 K.

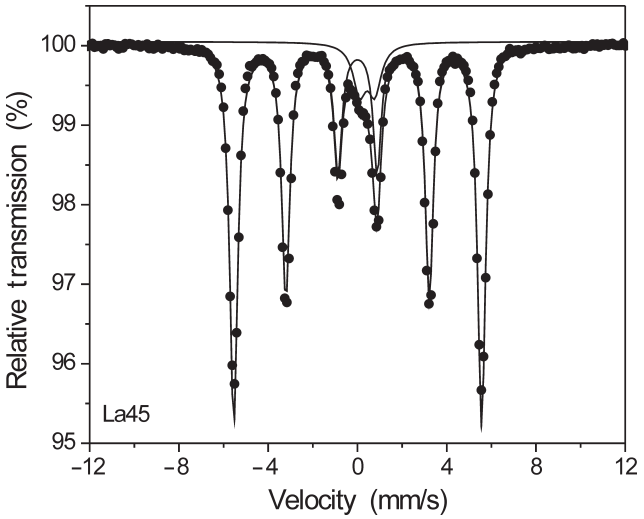

Fig. 10. Mössbauer spectrum of sample La45 after 30 days of iron-bentonite interactions, measured at 80 K.

tite account for 16 % and 13 % of the total Fe in the sample, respectively. The sextet with B_{hf} of 43.3 T could be attributed to goethite with partial substitution of Al for Fe in the structure. This phase accounted for 13 % of the total Fe in the sample. However, for more accurate mineral assignment the variable temperature Mössbauer spectroscopy should be applied. The sextet in the sample J45 assigned to residual metallic Fe accounted for only 17 % of the total Fe in the sample. This finding indicates that most of the metallic Fe reacted during iron-clay interaction and is chemically bonded.

The Fe in the sample DV45 also exists as metallic Fe in the quantity 18 % of the total Fe in the sample; however, in this sample more of the total Fe is bound in hematite and Al-hematite (total 38 %) compared to the sample J45 (Fig. 8, Table 2).

The Mössbauer spectrum of the sample K45 is similar to the spectrum of J45 (Figs. 7, 6). The most evident difference is that the metallic Fe in the sample K45 accounts for 46 % of the total Fe in the sample. Accordingly, the consumption of metallic Fe is much lower in the sample K45 with regard to the sample J45 during iron-clay interactions. The relative amount of metallic Fe in the iron phase is the lowest (12 %) in the sample L45 of all the studied samples (Table 2).

In the sample La45 only two Fe components are present — montmorillonite and residual metallic Fe (Table 2). The central doublet in the sample La45 is assigned to montmorillonite. This phase accounted for 9 % of the total Fe in the sample. The sextet in the sample is assigned to residual metallic Fe, which accounted for 91 % of the total Fe in the sample.

The Mössbauer spectroscopy revealed that in the samples J45, K45, DV45 and L45 the Fe was distributed among five Fe-bearing components, in the sample La45 only two Fe components were present (Table 2). The Mössbauer spectrum of the sample La45 was very different with respect to the Mössbauer spectra J45, K45, DV45 and L45. The other difference in spectra of particular samples was in the quantity of Fe in these Fe-bearing components. The residual metallic Fe accounted for 12–46 % of total Fe in the samples J45, K45, DV45 and L45, whereas 91 % of the total Fe was present as metallic Fe in the sample La45.

Cation exchange capacity

The results of cation exchange capacity (CEC) are given in Table 3. After iron-bentonite interactions the CEC values decreased in all samples. This change indicates the decrease in the content of expandable structure which might correspond to the decrease in the smectite content after the experiment. The decrease in CEC values was more significant with prolongation of the reaction time.

Solution chemistry

The results of AAS are summarized in Table 4. The conductivity, pH and Eh measured after cooling of the experimental solution at room temperature are given in Table 5. After 30 days solution pH was slightly alkaline between 7 and 8, Eh values ranged from −14 to +10 mV. After 30 days the concentrations of Si and Al were similar, Fe concentration was negligible in all samples. After 120 days all element concentrations increased (except for Al) in all samples.

Discussion

The results of FTIR spectroscopy and quantitative XRD analysis (RockJock) indicate the presence of volcanic glass in our samples. The presence of an absorption band at ~800 cm^{-1}

Table 3: Cation exchange capacities (meq/100 g) of starting samples (0 days) and samples after 30 and 120 days of iron-bentonite interactions.

Sample	0 days (meq/100g)	30 days (meq/100g)	120 days (meq/100g)
J45	97	91	87
L45	66	59	54
La45	71	63	n.a.
K45	102	83	85
DV45	35	30	25

Table 4: Chemistry of reaction solutions (in mg/l) after 30 and 120 days of iron-bentonite interactions determined by AAS (n.a. — not analysed).

Sample	Si (mg/l)	Al (mg/l)	Fe (mg/l)	Mg (mg/l)	Ca (mg/l)	Na (mg/l)	K (mg/l)
30 days							
J45	27.03	0.53	<0.265	12.19	117.66	351.92	230.02
L45	44.31	0.53	<0.265	6.04	69.43	203.52	155.82
La45	528.94	1.80	<0.265	22.26	111.30	789.70	85.97
K45	28.62	0.53	<0.265	10.39	58.51	474.88	147.34
DV45	15.69	0.64	<0.265	1.72	35.40	83.74	433.54
120 days							
J45	50.24	0.53	3.40	68.37	761.08	538.48	472.76
L45	74.41	0.53	8.17	60.42	770.62	499.26	486.54
La45	n.a.	n.a.	n.a.	n.a.	n.a.	n.a.	n.a.
K45	69.21	0.53	2.93	54.59	418.70	881.92	289.38
DV45	151.58	1.69	283.02	23.53	83.52	201.40	519.40

was assigned to the amorphous SiO_2 (Fig. 5). According to Číčel et al. (1992) the absorption band at ~800 cm^{-1} suggests the presence of Si bound in crystalline and/or non/crystalline phases like volcanic glass, opal, tridymite, cristobalite. Moreover, Číčel et al. (1990) observed differences in the structural formulas of montmorillonite from Jelšový Potok calculated from the acid dissolution and from bulk chemical analysis. These differences were attributed to the high extraneous SiO_2 amount in the sample. The authors observed that about one third of the mass of the sample was found to be extraneous to the montmorillonite and it was supposed that it is bound in feldspar and mainly in a volcanic glass. We determined the quantitative amount of cristobalite and volcanic glass in our samples from XRD patterns using the RockJock program. If the volcanic glass was included in the calculation of the mineral composition of bentonites, the degree of fit between measured and calculated XRD pattern was much better than the degree of fit when the volcanic glass was excluded from the calculation. This could be further circumstantial evidence of the presence of volcanic glass in the bentonite samples.

During the iron-bentonite interactions all experimental components may be altered and new mineral phases could be formed according to the published data. Magnetite and 1:1 Fe-rich 7 Å phyllosilicates (berthierine-like) are reported as the main reaction products of these interactions at a temperature of about 80 °C (Habert 2000; Lantenois 2003; Perronnet 2004; Lantenois et al. 2005; Wilson et al. 2006). Lantenois et al. (2005) and Perronnet et al. (2007) found that iron is oxidized in the presence of smectite, forming magnetite. Wilson et al. (2006) suggest that either green-rust or magnetite could be produced from the oxidation of iron.

The behaviour of the samples J45, K45, L45 during the experiments agrees with the published data. The lack of berthierine in our laboratory products could be explained by the aerobic experimental conditions. In fact, Harder (1978) found that Fe-containing clay minerals including 1:1 Fe-rich 7 Å phyllosilicates can be synthesized in a short time at low temperatures (~20 °C) but only under reducing conditions. Decrease of smectite diffraction peaks is a common feature of iron-clay interactions (Guillaume et al. 2003; Lantenois et al. 2005; Wilson et al. 2006). It may indicate decrease of smectite content (which means dissolution of smectite), split of smectite crystallites and/or smectite structural changes which result in a decrease of the number of coherently diffracting smectite domains.

We observed a clear decrease of the smectite XRD patterns intensity and CEC values after iron-bentonite interactions. These changes indicate the decrease in the smectite content after experiments. In contrast, FTIR spectra are the same before and after experiments, which implicitly indicates a process other than dissolution. As we did not identify any changes in FTIR spectra on the basis of Madejová et al. (1998) a study, which revealed that the FTIR spectroscopy is able to detect decrease in 10 % of structural Al in SWy-1 montmorillonite after acid treatment, we assumed that structural changes in smectites did not exceed 10 %. L45 bentonite contains Al–Fe^{3+} montmorillonite with the highest octahedral Fe^{3+} of all samples used for our experiments. However, there is no clear evidence that this smectite is destabilized more than smectites in samples J45, K45 and La45 (smectites with low structural Fe^{+3}). The conceptual model of smectite destabilization in the presence of iron was proposed by Lantenois et al. (2005). According to this model, destabilization of smectites resulting from the presence of trioctahedral (Fe^{2+}) domains in the octahedral sheet of reacted dioctahedral (Fe^{3+}) smectite, because of the inability of the tetrahedral sheet to accommodate the larger dimensions of the newly formed trioctahedral domains. The deprotonation of OH groups and the reduction of structural Fe^{3+} in the smectite are the main processes leading to the presence of trioctahedral (Fe^{2+}) domains in the dioctahedral (Fe^{3+}) smectite structure. Apparently no sign of these changes was detected by the XRD, FTIR and Mössbauer spectroscopy in our samples. It indicates that aerobic experimental conditions prevent the above mentioned processes in the system.

The formation of small amounts of lepidocrocite instead of magnetite in the sample La45 after the experiment (Fig. 3) could be explained by more oxidizing conditions (the highest Eh value of all samples) in comparison with the other samples (Table 5). It means that the Fe^{2+} produced by oxidation of iron was oxidized very fast to Fe^{3+} therefore the concentration of Fe^{2+} ions in the reaction solution was too low for magnetite formation. Lantenois (2003) used XRD to identify lepidocrocite as the by-product of the air exposure of the Fe-containing gel phase after iron-clay interactions at 80 °C.

The very low level of Fe oxidation in the sample La45 in respect to the other bentonites is a surprise. The low reactivity between bentonite La45 and iron may be connected with a different mineral composition of the bentonite La45 with respect to the bentonites J45, L45 and K45 (Table 1). The bentonite La45 contains 42 % of smectite while the smectite content in bentonites J45, L45 and K45 is much higher (56–81 %). We suppose that the very low smectite content in the bentonite La45 could be the reason for low reactivity with iron.

This assumption is consistent with the observations of Perronnet (2004), Lantenois et al. (2005) and Perronnet et al. (2007) who found that iron is not consumed (oxidized) in the absence of smectite whereas in the presence of smectite, iron is oxidized. The high affinity of iron for smectite followed by iron-smectite interactions have been recognized as the cause of oxidation of steel pipes when clay-containing drilling fluids were used (Tomoe et al. 1999; Cosultchi et al. 2003).

Another interesting feature is the drastic deterioration of the illite-smectite from the Dolná Ves deposit. In DV45 sample the iron was consumed, magnetite was formed, the diffraction peaks of illite-smectite decreased significantly after the experiment and a new diffraction peak of smectite was detected (Fig. 4). The results of infrared spectroscopy showed decrease in intensities of OH-bending vibrations, which reflect release

Table 5: The properties of reaction solutions measured (at room temperature) after 30 days of iron-bentonite interactions.

Sample	pH	Eh (mV)	Conductivity (μS/cm)
Redistilled water	5.70	170	5.92
J45	7.59	–10	242
L45	7.30	+10	144
La45	7.94	+78	330
K45	7.77	+10	241
DV45	7.10	–14	144

of the central atoms (Al, Mg) from the octahedral sheet of illite-smectite after the experiment. The decrease in CEC values indicates the decrease in the illite-smectite content after the experiment. It is clear from the XRD, FTIR and CEC that experimental interactions caused dissolution of the original illite-smectite. The delamination of illite-smectite crystals can be excluded because it would have resulted in the shift of XRD peaks (delamination would change the ratio of expandable and non-expandable layers). It seems that the illite-smectite with its significantly lower surface area (1/3 of smectite) is much less resistant to the experimental conditions than the smectites.

The concentrations of alkali and alkali-earth cations, which were initially present in smectite interlayers (Ca^+, Na^+, Mg^{2+}, K^+), were significantly higher after 120 days. This increase is probably the result of exchange processes between smectite interlayer cations and cations contained in reaction solution. Increase in Si and Mg concentrations could be related to the changes in the smectite structure, and higher Si concentrations may also be related to quartz and feldspar dissolution during iron-clay interactions. High Si concentration in the sample La45 after 30 days can be explained by dissolution of amorphous SiO_2 (volcanic glass, cristobalite) during iron-clay interactions. It is in accordance with XRD data, because after iron interactions the diffraction peak of cristobalite disappeared in the sample La45 after 30 days. Significant increase in Fe content in all samples after 120 days could be explained by changes in the oxidation state of iron and the subsequent mobilization of the iron.

Conclusions

The experiments compared with the previously published data show that bentonites do not react with iron in aerobic environment in the same way as in anaerobic environments.

Three smectitic bentonites — J45, K45, and L45, had very similar or almost identical reactions. The diffraction peaks of smectite decreased but were still clearly visible in XRD patterns. The iron was consumed to a large extent and magnetite was formed (Fig. 2). In the sample La45 the intensity of diffraction peaks of smectite decreased but the iron was much less consumed (oxidized) during iron-clay interactions and instead of magnetite a small amount of lepidocrocite was formed (Fig. 3). The fact that iron oxidation was prevented in La45 can be explained by the low content of smectite.

Significant decrease of the smectite XRD patterns intensity and CEC values during the experiments cannot be assigned to the dissolution of smectite. It represents, rather, a rearrangement of the original smectite crystals.

Mixed-layer illite-smectite proved to be much less stable in the presence of iron than smectites. Clear signs of I-S dissolution were detected along with the neoformation of smectite.

Acknowledgments: The authors are grateful to Dr. Peter Komadel for constructive comments and help during preparation of the paper. This study was supported by the Slovak Grant Agency VEGA (Projects 1/3072/06 and 2/0171/08) and by the Student Research Grant UK/272/2008.

References

Arthur R., Apted M. & Stenhouse M. 2005: Comment on Long-Term Chemical and Mineralogical Stability of the Buffer. *SKI Report 2005:09, Swedish Nuclear Power Inspectorate*, Stockholm, Sweden.

Betancur J.D., Barrero C.A., Greneche J.M. & Goya G.F. 2004: The effect of water content on the magnetic and structural properties of goethite. *J. Alloys. Compounds* 369, 247–251.

Börgesson L., Karnland O., Hökmark H. & Sellin P. 2002: Buffer and Safety Assessment for KBS-3H. SKB, September 2002.

Cosultchi A., Rossbach P. & Hernandez-Calderon I. 2003: XPS analysis of petroleum well tubing adherence. *Surface and Interface Analysis* 35, 239–245.

Číčel B., Komadel P. & Hronský J. 1990: Dissolution of the fine fraction of Jelšový Potok bentonite in hydrochloric and sulphuric acids. *Ceramics* 34, 41–48.

Číčel B., Komadel P., Bednáriková E. & Madejová J. 1992: Mineralogical composition and distribution of Si, Al, Fe, Mg and Ca in the fine fractions of some Czech and Slovak bentonites. *Geol. Carpathica, Ser. Clays* 43, 1, 3–7.

Eberl D.D. 2003: User's guide to Rockjock — a program for determining quantitative mineralogy from powder X-ray diffraction data. *U.S. Geol. Surv., Open-File Report* 03–78, 47.

Friedl J. & Schwertmann U. 1996: Aluminium influence on iron oxides: XVIII. The effect of Al substitution and crystal size on magnetic hyperfine fields of natural goethites. *Clay Miner.* 31, 455–464.

Golden D.C., Bowen L.H., Weed S.B. & Bigham J.M. 1979: Mössbauer studies of synthetic and soil-occurring aluminum-substituted goethites. *Soil Sci. Soc. Amer. J.* 43, 802–808.

Guillaume D., Neaman A., Cathelineau M., Mosser-Ruck R., Peiffert C., Abdelmoula M., Dubessy F., Villiéras F., Baronnet A. & Michau N. 2003: Experimental synthesis of chlorite from smectite at 300 °C in the presence of metallic Fe. *Clay Miner.* 38, 281–302.

Guillaume D., Neaman A., Cathelineau M., Mosser-Ruck R., Peiffert C., Abdelmoula M., Dubessy F., Villiéras F. & Michau N. 2004: Experimental study of the transformation of smectite at 80 °C and 300 °C in the presence of Fe oxides. *Clay Miner.* 39, 17–34.

Habert B. 2000: Réactivité du fer dans les gels et les smectites. *Thesis*, Université Paris 6, Paris, 1–227.

Harder H. 1978: Synthesis of iron layer silicate minerals under natural conditions. *Clays Clay Miner.* 26, 1, 65–72.

JNC 2000: Second progress report on research and development for the geological disposal of HLW in Japan. H12: Project to establish scientific and technical basis for HLW disposal in Japan (Project Overview Report). JNC TN1410 2000-001.

Kaufhold S. & Dohrmann R. 2003: Beyond the methylene blue method: determination of the smectite content using the Cu-Triene method. *Z. Angew. Geol.* 2, 13–17.

Lantenois S. 2003: Réactivité fer métal/smectites en milieu hydraté à 80 °C. *Ph.D. Thesis*, Université d'Orléans, Orléans, 1–188.

Lantenois S., Lanson B., Muller F., Bauer A., Jullien M. & Plançon A. 2005: Experimental study of smectite interaction with metal Fe at low temperature: 1. Smectite destabilization. *Clays Clay Miner.* 53, 6, 597–612.

Madejová J., Bujdák J., Janek M. & Komadel P. 1998: Comparative FT-IR study of structural modifications during acid treatment of dioctahedral smectites and hectorite. *Spectrochimica Acta, Part A*, 54, 1397–1406.

Madejová J., Kečkéš J., Pálková H. & Komadel P. 2002: Identification of components in smectite/kaolinite mixtures. *Clay Miner.* 37, 377–388.

Madsen F.T. 1998: Clay mineralogical investigations related to nu-

clear waste disposal. *Clay Miner.* 33, 109–129.

Meier L.P. & Kahr G. 1999: Determination of the cation exchange capacity (CEC) of clay minerals using the complexes of copper(II) ion with triethylentetramine and tetraethylenepentamine. *Clays Clay Miner.* 47, 386–388.

Müller-Vonmoos M., Kahr G., Bucher F., Madsen F.T. & Mayor P.A. 1991: Untersuchungen zum Verhalten von Bentonit in kontakt mit Magnetit und Eisen unter Endlagerbedingungen. NTB 91-14. Nagra, Hardstrasse 73, CH-5430, Wettingen, Switzerland.

Murad E. 1988: Properties and behaviour of iron oxides as determined by Mössbauer spectroscopy. In: Stucki J.W., Goodman B.A. & Schwertmann U. (Eds.): Iron in soils and clay minerals. *Reidel*, Dordrecht, 309–350.

Murad E. 1989: Poorly-crystalline minerals and complex mineral assemblages. *Hyperfine Interactions* 47, 33–53.

Perronnet M. 2004: Etude des interactions fer-argile en condition de stockage géologique profond des déchets nucléaires HAVL. *Ph.D. Thesis*, *ENS Géologie*, Nancy, 1–233.

Perronnet M., Villiéras F., Jullien M., Razafitianamahavaro A., Raynal J. & Bonnin D. 2007: Towards a link between the energetic heterogeneities of the edge faces of smectites and their stability in the context of metallic corrosion. *Geochim. Cosmochim. Acta* 71, 1463–1479.

Push R. 2001: The Buffer and Backfill Handbook. Part 2: Materials and techniques. SKB TR 02-12. *Swedish Nuclear Fuel and Waste Management Co*., Stockholm, Sweden.

Push R. 2003: The Buffer and Backfill Handbook. Part 3: Models for calculation of processes and behavior. SKB TR 03-07. *Swedish Nuclear Fuel and Waste Management Co*., Stockholm, Sweden.

SKI 2005: Engineered barrier system — Long-term stability of buffer and backfill. SKI Report 2005:48. *Swedish Nuclear Power Inspectorate*, Stockholm, Sweden.

Smart N.R., Blackwood D.J. & Werme L. 2002: Anaerobic corrosion of carbon steel and cast iron in artificial groundwaters: Part 1 — Gas generation. *Corrosion* 58, 627–637.

Środoń J., Drits V.A., McCarty D.K., Hsieh J.C.C. & Eberl D.D. 2001: Quantitative X-ray diffraction analysis of clay-bearing rocks from random preparations. *Clays Clay Miner.* 49, 6, 514–528.

Thorsager P. & Lindgren E. 2004: KBS-3H — Summary report of work done during basic design. SKB Rapport R-04-42. *Swedish Nuclear Fuel and Waste Management Co*., Stockholm, Sweden.

Tomoe Y., Shimizu M. & Nagae Y. 1999: Unusual corrosion of a drill pipe in newly developed drilling mud during deep drilling. *Corrosion* 55, 706–713.

Wilson J., Cressey G., Cressey B., Cuadros J., Vala Ragnarsdottir K., Savage D. & Shibata M. 2006: The effect of iron on montmorillonite stability. (II) Experimental investigation. *Geochim. Cosmochim. Acta* 70, 323–336.